Int. J. Heat Mass Transfer. Vol. 26, No. 7, pp. 1007–1016, 1983
Printed in Great Britain

0017-9310/83 $3.00 + 0.00
Pergamon Press Ltd.

EXPERIMENTAL STUDY OF MASS TRANSFER AROUND A TURBULENCE PROMOTER BY THE LIMITING CURRENT METHOD

DO HYUN KIM, IN HO KIM and HO NAM CHANG*

Department of Chemical Engineering, Korea Advanced Institute of Science and Technology, P.O. Box 150 Chongyangni, Seoul, Korea

(*Received* 15 *April* 1982 *and in revised form* 4 *November* 1982)

Abstract—Local mass transfer rates around a turbulence promoter in a channel having the geometry of zigzag-type or cavity-type characterized by the location of promoters have been measured by the limiting current technique.

The experimental results showed that turbulence promoters are effective in breaking the concentration boundary layer and thus increasing the mass transfer rate. In the present experiment the Reynolds numbers were varied from 10 to 200 for the different aspect ratios of 3.5, 5 and 7. The experimentally obtained Sherwood numbers were compared with those numerically obtained by Kang and Chang. As a result, they were found to be in agreement to within an error of 20%.

NOMENCLATURE

- AR, aspect ratio, L/H;
- C_0, bulk concentration;
- D, diffusivity;
- F, Faraday's constant (96487 C equiv^{-1});
- H, channel height;
- i_{lim}, limiting current density;
- k, mass transfer coefficient;
- L, distance between the centers of successive promoters;
- Pe, Péclet number, $U_{av}H/D$;
- Re, Reynolds number, $U_{av}H\rho/\mu$;
- Sc, Schmidt number, $\mu/\rho D$;
- Sh, Sherwood number, kH/D;
- U_{av}, mean velocity of flow in the channel;
- z, number of electrons exchanged during electrode reaction.

Greek symbols

- μ, viscosity;
- ρ, density of fluid.

1. INTRODUCTION

IN ORDER to promote mass transfer between a fluid and a solid it is necessary to fully understand the nature of the governing boundary layers. Usually the solute concentration remains very low or nearly zero at the solid or membrane surfaces where rapid depletion of solute takes place owing to chemical reaction or membrane transport. In this case the solute transport from the bulk fluid to the solid surfaces becomes rate limiting.

When the fluid enters the mass transfer region in a channel, the diffusion layer begins to grow, where the solute concentration varies from that of the bulk fluid to that on the surface. As a result, the mass transfer to the surface is gradually retarded along the fluid path. One method of increasing the mass transfer rate in such a situation is to interrupt the continuous growth of the diffusion layer near the wall by placing turbulence promoters in the channel.

Spacers used for electrodialysis and in artificial kidneys play the role of turbulence promoter as well as being spacers and supports on the membranes. The spacers for electrodialysis are generally classified into two types. One is known as the tortuous path type and the other utilizes the principle of sheet flow [1]. To investigate the enhanced mass transfer effect of spacers for electrodialysis, Solan *et al.* [2] proposed the analytical mesh step model and Kang and Chang [3] numerically analyzed the hydrodynamic performance of the zigzag-type and cavity-type spacers, characterized by the location of the promoters. Experimental criteria to evaluate the hydrodynamic performance of industrial electrodialysis spacers were also provided [4] and their influence on the product cost was investigated [5, 6]. In addition, in connection with electrodialysis, mass transfer studies around the attached [7] and detached [8] cylindrical promoter were also carried out.

In most cases when turbulence promoters are used, mass transfer is augmented by recirculating flow formed before or behind the promoters. Recirculating flows are also formed in the flows over a semi-cylindrical hollow [9] and near an entry of abrupt expansion [10–12], which all result in the increase of mass transfer. All these studies employed the limiting current technique in common in measuring the local mass transfer rates and lacked rigorous theoretical analyses. Therefore the present study aims at experimentally confirming the results of the numerical analysis performed in our laboratory [3] by varying the Reynolds numbers and the aspect ratio of the zigzag- or cavity-type promoters.

2. EXPERIMENTAL TECHNIQUE

The limiting current technique is widely used in recent years for heat and mass transfer study, which measures a current density at a cathode where the

* To whom all correspondence should be addressed.

reduction of ferricyanide ion takes place. The advantage of the limiting current technique over the formerly used metal deposition or solid dissolution method is that the surface where mass transfer occurs is not physically changed and the steady state electrode potential can be attained much faster than in the metal deposition reaction. This enables us to make instantaneous measurements. Besides, local mass transfer rate can be measured with tiny electrodes. The details of the limiting current technique may be found elsewhere [13–18]. From the current measurements the mass transfer coefficient, k, is given by

$$k = i_{lim}/zFC_0. \quad (1)$$

The dimensionless mass transfer rate, the Sherwood number can be expressed as

$$Sh = kH/D = i_{lim}H/zFC_0D \quad (2)$$

where H is a characteristic length and represents the channel height in this system.

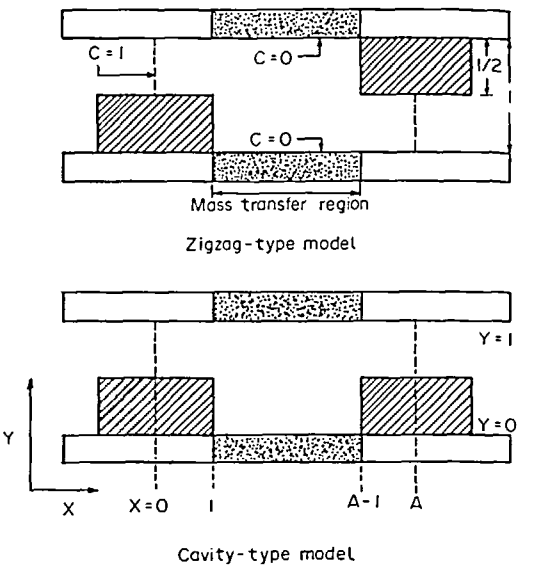

FIG. 1. Modelled systems for turbulence promoters.

3. APPARATUS

3.1. *The flow circuit*

The schematic diagrams of the model promoters and the flow circuit used in the present study are given in Figs. 1 and 2, respectively. The electrolyte was pumped through a flow damper, gas trap and finally into a test cell. The flow damper attenuates the pulsation generated by a pump and prevents gas bubbles from entering the test cell. The plastic net placed at the triangular entry section of the test cell provided uniform flow of the electrolyte. The upper and lower plates of the test cell were made of 1 cm thick lucite plate. A cathode package was installed in the upper plate and an anode in the lower plate. Two rubber sheets of 3 mm thickness, parts of which were cut out to provide a flow path, were overlapped to play the role of the cavity-type or zigzag-type promoters. Since the flow patterns characterizing the system are developed immediately after a few stages of promoters, the cathodes were placed at the third and the seventh stages for those with the aspect ratio of 7 and 3.5, respectively. The rectangular cross-section of the test cell was 80 mm wide and 6 mm high, and thus the flow could be assumed as two-dimensional. The upper and lower plates of the test cell were made easily interchangeable. The supporting steel plates were attached on both sides

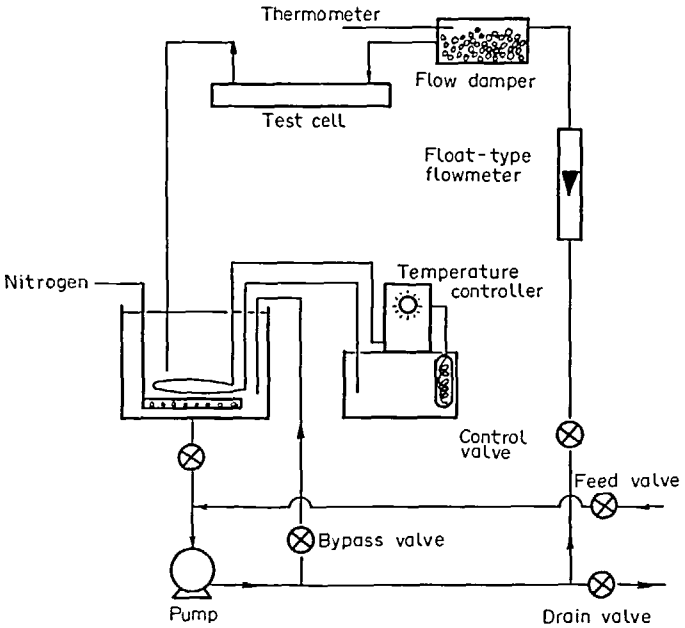

FIG. 2. Schematic arrangement of experimental equipment.

of the test section to ensure uniform distribution of tension over the entire area. Flow rate was measured by a rotameter (model B362, Roger Gilmont Instruments, Great Neck, NY). The solution collected in the tank was pumped back through a Tygon tubing to a test cell by a controllable gear pump (model 12-41-316, Micro-pump, Concord, CA).

3.2. *The electrodes*

All electrodes were made of nickel strips which were sandwiched to form a cathode package. Copper wires were silver-soldered to each of the electrodes.

Mica, having the same dimensions as the electrodes, was inserted between the adjacent electrodes to ensure electrical isolation and fixed together with epoxy resin. Consequently the cathodes and the mica form an alternating pattern of an electrically active region followed by an inert region. In this study the ratio of length of the active region (cathode) to that of the inert region (mica) in the flow direction was 4.2. A large rectangular anode, 50 mm long and 60 mm wide, was mounted at the downstream end of the lower plate.

Since the surface condition of the electrode has a significant influence on the limiting current, the electrode surface was polished with fine emery paper to remove any oxide film. This was followed by washing with detergent and carbon tetrachloride to remove the oil film. To activate the electrodes, cathodic treatment [14, 16] was performed by placing the electrodes in 2 M NaOH solution and applying a negative potential for 4–5 min. The same cathode package was used throughout the experiment.

3.3. *Current measurement*

The simplified circuit is shown in Fig. 3. Potential was not applied to the electrode shadowed by the promoter to satisfy the boundary condition depicted in Fig. 1. A switch box was made to measure current from a single strip without being influenced by other strips. The currents were measured using a digital multimeter (Model 619, Keithley, Cleveland, OH) and the supply voltage was measured at the probe of a power supply (Model 6214A, Hewlett Packard, Loveland, CO) by a digital multimeter (Model 160B, Keithley). When the currents fluctuated, they were made to pass through a 4.79 ohm resistor and the voltage across the resistor was recorded by a dual-pen chart-recorder.

Table 1. Properties of electrolytic solution composed of 0.01 M $K_3Fe(CN)_6$, 0.01 M $K_4Fe(CN)_6$ and 1.0 M NaOH

	Measured	From literature†
Density	1.044 g cm^{-3}	1.0426 g cm^{-3}
Viscosity	1.1004 cp	1.1021 cp
Diffusivity‡		6.37 × 10^{-6} cm^2 s^{-1}

† Ref. [23].
‡ Diffusivity of ferricyanide ion.

3.4. *Electrolytic solution*

The electrolytic solution used in the present study consisted of the following mixture: 0.01 M of $K_3Fe(CN)_6$, 0.01 M of $K_4Fe(CN)_6$ and 1.0 M of NaOH. Because the limiting current measured is directly proportional to the bulk concentration of ferricyanide ion, it is important to know this concentration precisely. The concentrations were checked periodically using an iodometric method [19] for ferricyanide and permanganate titration [20] for ferrocyanide. Decomposition of ferrocyanide proceeds in the light even without oxygen to form aquopentacyanide [21]. This reaction contaminates the solution as well as deactivating the electrode surface. To remove this effect, the tank was painted on the surface to avoid direct exposure to the ultraviolet light and Tygon tubings were shielded with aluminum foil. Since the presence of dissolved oxygen in the electrolytic solution had an adverse effect upon the electrochemical reaction [22], nitrogen was bubbled through the solution for 2 h at 5 l min^{-1} before measurement and at 2 l min^{-1} throughout all the runs to eliminate dissolved oxygen.

As the properties of the solution, particularly the

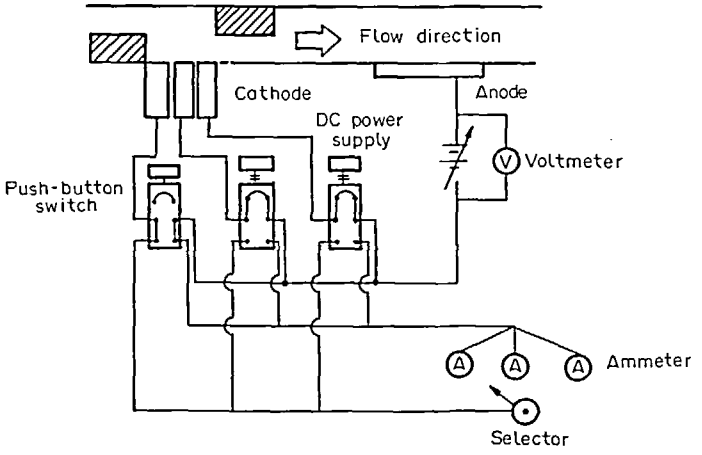

FIG. 3. Simplified electric circuit diagram.

diffusivity of the electrolyte, are dependent on the temperature, the temperature of the solution was maintained at $25 \pm 0.3°C$ by circulating water to the solution tank. In addition to this, temperature was also checked in the flow damper before the solution enters the test cell. The density of the sample solution was measured using a hydrometer and the viscosity using a Ubbelohde pipette. The properties of the electrolyte using semi-empirical equations are well summarized in the ref. [23] (see Table 1).

4. RESULTS AND DISCUSSION

4.1. *Comparison of zigzag-type and cavity-type promoter*

Polarization curves similar to Fig. 4 were obtained from the experiment. The limiting current plateau always appeared at Reynolds numbers below 200, but at Reynolds numbers above 300 the current often began to fluctuate.

The experimental local Sherwood numbers in the first stage and the second stage of each geometry are presented in Fig. 5 in order that the performance characteristics of the zigzag-type and cavity-type promoter may be compared. Throughout the study, a lower wall for a zigzag-type promoter means a region behind a promoter and upper wall before a promoter, while a lower wall for a cavity-type promoter refers to a region where promoters are installed and upper wall refers to a wall without promoters.

In the presence of a turbulence promoter, recirculating flows are formed in front of and behind a promoter, the shear rate at the wall increases and the concentration boundary layers are broken periodically. Consequently the Sherwood number distributions for the zigzag-type promoter do not show a great difference between the first and second stage. However, on the upper wall for the cavity-type promoter, the concentration boundary layer keeps growing, resulting in a continuous decrease in the mass transfer rate stage by stage, as can be seen in Fig. 5. The performance of the zigzag-type promoter is considered better than that of the cavity type in breaking the concentration boundary layer and thus bringing about an increase in mass transfer.

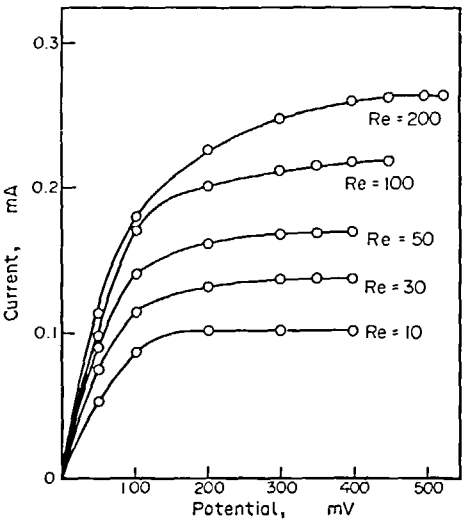

FIG. 4. Polarization curve for the reduction of ferricyanide (zigzag-type, upper wall, electrode No. 6).

4.2. *Local Sherwood number distribution*

Sherwood number distributions in the first stage for the zigzag-type promoter vs dimensionless distance X are shown in Figs. 6–9. In the present study, strip

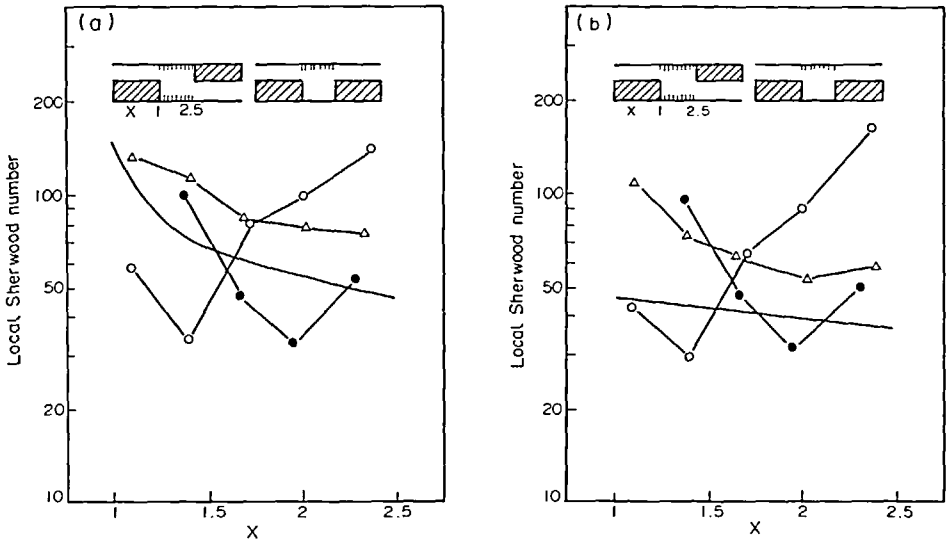

FIG. 5. Sherwood number distributions at first and second stage with and without turbulence promoter ($AR = 3.5, Re = 100$). (a) First stage. (b) Second stage. Zigzag-type lower wall, ○. Zigzag-type upper wall, ●. Cavity-type upper wall, △. —— empty channel.

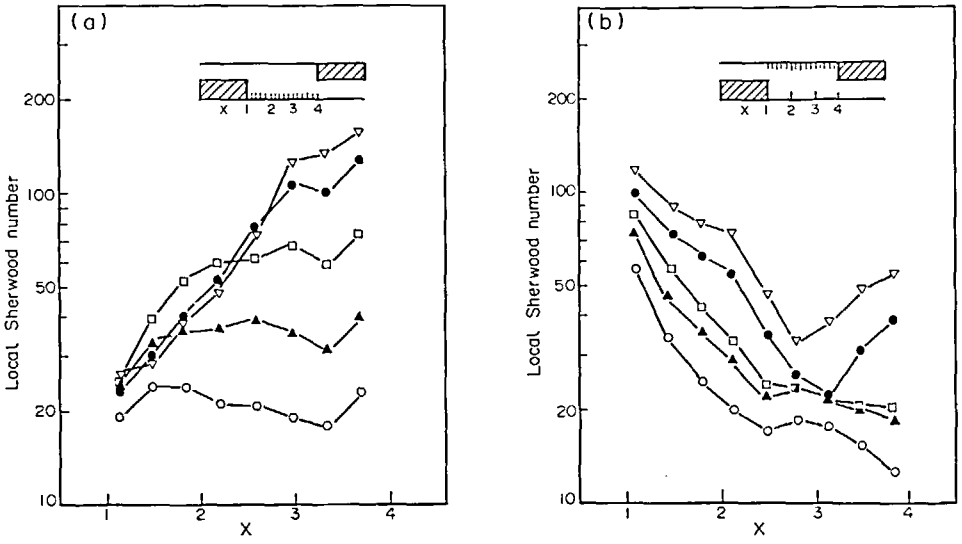

FIG. 6. Local Sherwood number distributions ($AR = 5$, zigzag-type, first stage). (a) Lower wall. (b) Upper wall. $Re = 10$, ○; $Re = 30$, ▲; $Re = 50$, □; $Re = 100$, ●; $Re = 200$, ▽.

electrodes are used. Thus symbols represent the value which is an average Sherwood number on the strip electrode.

The local Sherwood number distribution on the wall for the zigzag-type promoter of aspect ratio 5 is shown in Fig. 6(a) with the Reynolds number as a parameter. The mass transfer region and the associated coordinates are shown in the upper part of Fig. 6(a). The range in which mass transfer arises becomes longer as the Reynolds number increases. This indicates that the eddy size of recirculating flow is important in enhancing the mass transfer at the wall [3]. Figure 6(b) shows the local Sherwood number distribution on the upper wall in the same flow path. After the fluid passes through a narrow gap above a promoter, a recirculating flow immediately forms behind the promoter. But on the opposite wall the concentration boundary layer keeps growing and the mass transfer rate decreases until the fluid encounters the promoter and a recirculating flow forms in front of the promoter which is smaller in eddy size than that formed behind the promoter. As can be seen in Fig. 6(b), at Reynolds numbers below 50, the recirculating flow has not yet created any eddy large enough to influence the mass transfer, and the mass transfer rate decreases along the path. However, at Reynolds numbers above 100, recirculating flows with considerable eddy size are formed in front of the promoter [3] and the mass transfer rate was observed to increase in the recirculation zone.

The local Sherwood number distributions for the cavity-type promoters are shown in Figs. 7(a) and 7(b).

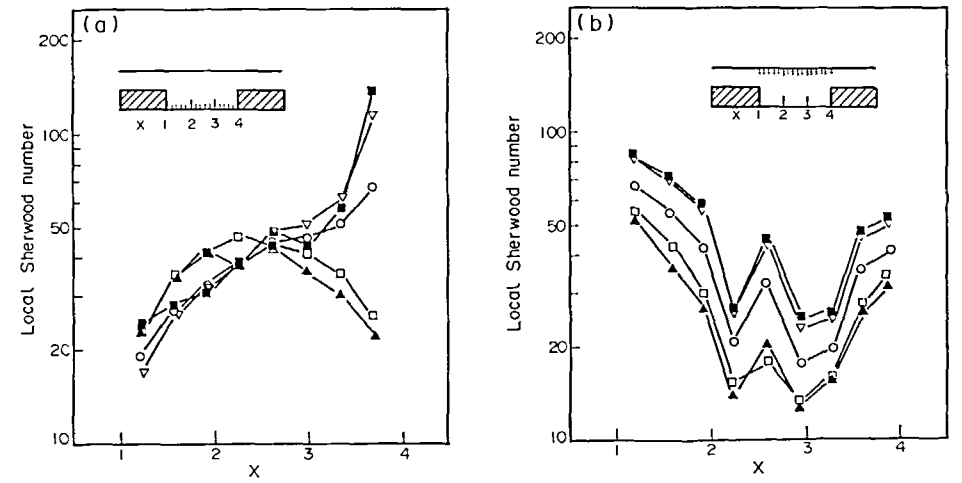

FIG. 7. Local Sherwood number distributions ($AR = 5$, cavity type, first stage). (a) Lower wall. (b) Upper wall. $Re = 30$, ▲; $Re = 50$, □; $Re = 100$, ○; $Re = 200$, ▽; $Re = 300$, ■.

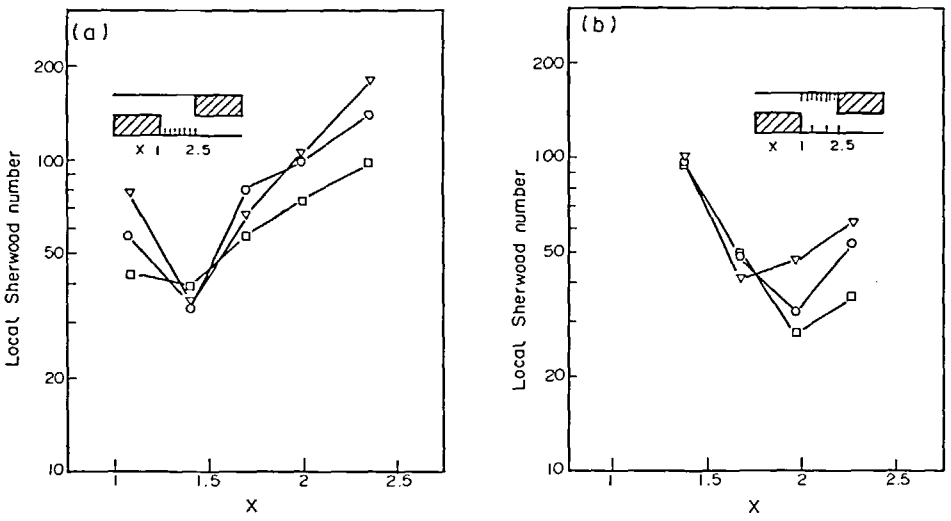

FIG. 8. Local Sherwood number distributions ($AR = 3.5$). (a) Zigzag-type, first stage, lower wall. (b) Zigzag-type, first stage, upper wall. $Re = 50$, □; $Re = 100$, ○; $Re = 200$, ▽.

In Fig. 7(a), the region of increasing Sherwood numbers extended to the full mass transfer area with increasing Reynolds number. The peak Sherwood numbers around $X = 2.5$ in Fig. 7(b) contradict the numerical predictions of Kang and Chang [3], which are lower than those at $X = 2.2$ and $X = 2.9$. However, these data were included owing to the reproducible nature of the experimental results.

The local Sherwood number distributions for the zigzag-type promoter of $AR = 3.5$ are shown in Figs. 8(a) and 8(b) and those of $AR = 7$ in Figs. 9(a) and 9(b). The same cause and effect for the Reynolds number as in the case of $AR = 5$ can be observed in these figures.

4.3. *Comparison of the experiment with the numerical analysis*

Figures 10(a)–(d) show a comparison of the Sherwood numbers from the experiments with those predicted from the numerical analysis. In this study, the same grid size and finite-difference numerical technique used by Kang and Chang [3] were employed. The concentration profile near the wall was assumed to be of three types, linear, a second order and a third order polynomial, from which the dimensionless derivative evaluated at the wall was taken as the Sherwood number. The linear approximation was closest to the experimental value and the second order profile gave

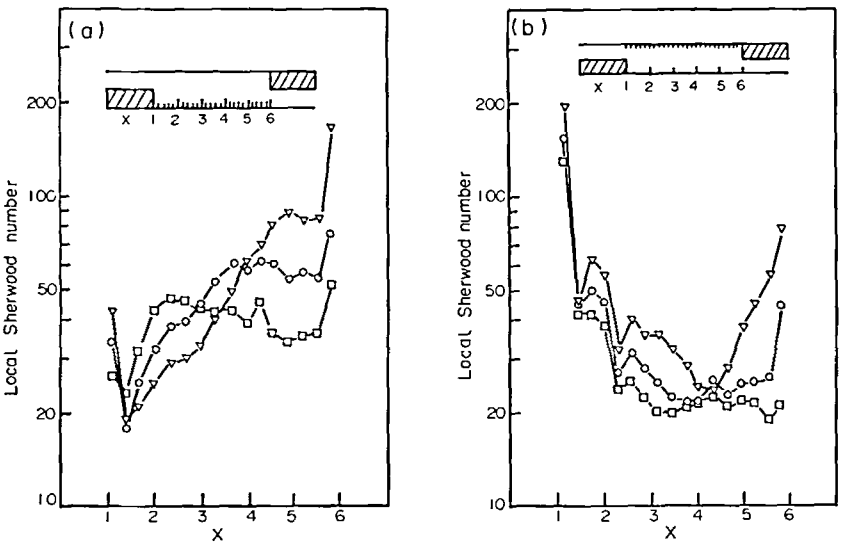

FIG. 9. Local Sherwood number distributions ($AR = 7$). (a) Zigzag-type, first stage, lower wall. (b) Zigzag-type, first stage, upper wall. $Re = 50$, □; $Re = 100$, ○; $Re = 200$, ▽.

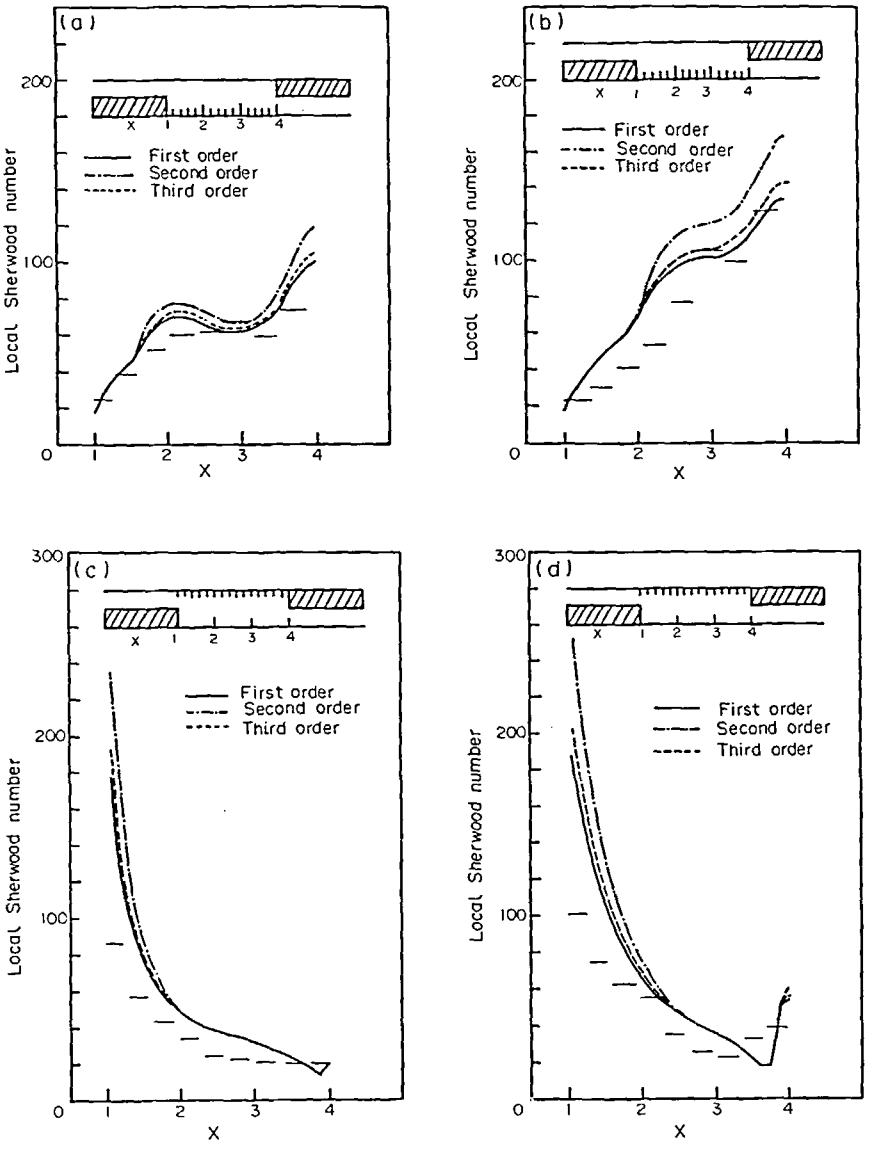

FIG. 10. Comparison with numerically calculated Sherwood number ($AR = 5$). (a) Zigzag-type, first stage, lower wall, $Re = 50$, (b) zigzag-type, first stage, lower wall, $Re = 100$, (c) zigzag-type, first stage, upper wall, $Re = 50$, (d) zigzag-type, first stage, upper wall, $Re = 100$.

higher Sherwood numbers than the other two approximations.

Although the experimental Sherwood number distributions show a similar trend to the results of the numerical analysis, a deviation of 10–20% in the absolute values was observed at some points of Figs. 10(a)–(d). One reason for this is that the upwind difference scheme employed in the numerical analysis gives accurate values at small Péclet numbers, and the solution from this has a tendency to deviate from the exact solution at large Péclet numbers. This can be confirmed by the fact that the numerical results become closer to the experimental Sherwood number at a Reynolds number of 50 [Figs. 10(a) and 10(c)], than at a Reynolds number of 100 [Figs. 10(b) and 10(d)].

4.4. *Mean Sherwood number*

In the channel with turbulence promoters, the mean Sherwood number over the mass transfer region can be expressed as a function of the Reynolds number, the Schmidt number and the aspect ratio from the result of dimensional analysis. In the present study the Schmidt number was fixed as 1690 since the composition of the solution was fixed and the temperature of the solution was maintained at a constant value of 25°C. Consequently, the dependency of the mean Sherwood number on the Reynolds number and aspect ratio was investigated for the zigzag-type promoter. The form of $Sh = Re^x AR^y$ was chosen for the Sherwood number correlation and the x and y values were obtained from a multilinear regression. As a result, the correlations are

expressed in the form $Sh_m = 31.6\,Re^{0.420}AR^{-0.776}$ for the lower wall and $Sh_m = 24.6\,Re^{0.327}AR^{-0.527}$ for the upper wall as shown in Fig. 11. From these it can be deduced that the mean Sherwood number in the channel with turbulence promoters increases faster at the lower wall ($x = 0.420$) than at the upper wall ($x = 0.327$) with the Reynolds number, which is consistent with Levich's findings [24]. Contrary to the dependence on the Reynolds number, it decreases with the aspect ratio, which favorably compares with the experimental correlation ($y = -0.5$) obtained by Sonin and Isaacson [5]. However, in electrodialysis systems, a decrease of aspect ratio results in an increase in current blockage due to the presence of spacer which reduces the overall efficiency. In view of this, the optimum aspect ratio is said to be 4–5 [5, 6]. For practical electrodialytic spacers, an aspect ratio of 10 was used for the tortuous path design spacer by Ionics Co., 4.93 and 5.33 for the spacers used in brine compartments and dialysate compartments, respectively, by Hanjoo Salt Co. (Ulsan, Korea), and 3.75 for the net spacer in artificial kidneys. All these are in the aspect ratio range 3.5–5.5 except the tortuous-path design spacer.

Although the mean Sherwood number increases with the Reynolds number, for large Reynolds numbers above 10^3, the excessive pumping costs in comparison with the improvement in the mass transfer efficiency should be considered. Accordingly, the optimum Reynolds number was reported to fall in the range 10^2–10^3 [5].

The overall mean Sherwood number for both the lower and upper wall of the zigzag-type promoter can be correlated as

$$Sh_m = 27.9\,Re^{0.376}AR^{-0.656}. \qquad (3)$$

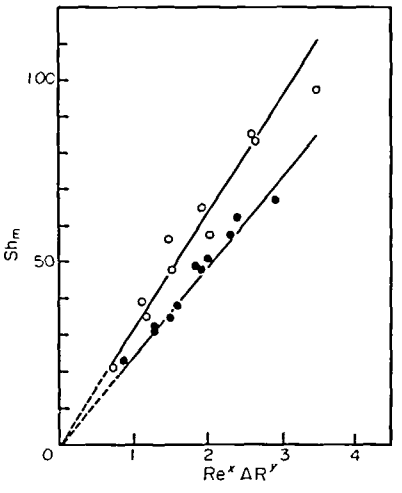

FIG. 11. Correlations for mean Sherwood number as a function of Reynolds number and aspect ratio (zigzag-type, $Sc = 1690$). $Re = 10$–200, $AR = 3.5$, 5 and 7. ○, lower wall, slope = 31.6, $x = 0.420$, $y = -0.776$. ●, upper wall, slope = 24.6, $x = 0.327$, $y = -0.527$.

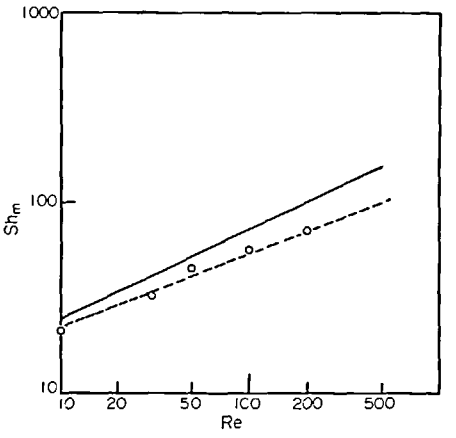

FIG. 12. Comparison of the experimental data with the numerically predicted value. ——— Numerical result. — — — Experimental result.

The correlation obtained numerically by Kang and Chang [3] using the second-order concentration profile near the wall is

$$Sh_m = 0.519\,Re^{0.475}\,Sc^{0.376}. \qquad (4)$$

The Sherwood numbers evaluated from equations (3) and (4) are compared in Fig. 12 using the values $AR = 5$ and $Sc = 1690$. The deviation between the two is about 6% at $Re = 10$ and 20% at $Re = 200$. If equation (4) had been obtained from the linear approximation instead of the second order one, it is clear from Figs. 10(a)–(d) that the deviation between the two would have been smaller.

5. CONCLUSIONS

The zigzag-type turbulence promoter has been shown to be more effective than the cavity-type promoter in breaking the concentration boundary layer and thus increasing the mass transfer rate. The local mass transfer rate was greatly influenced by the formation of recirculating flows in front of and behind a turbulence promoter. The unsteady nature of turbulence caused by the turbulence promoter brought about current fluctuation at Reynolds numbers above 300.

The mean Sherwood number was correlated for the zigzag-type promoter with $Sc = 1690$, giving the final form of the Sherwood number as

$$Sh_m = 31.6\,Re^{0.420}AR^{-0.776} \quad \text{for the lower wall,}$$

$$Sh_m = 24.6\,Re^{0.327}AR^{-0.527} \quad \text{for the upper wall,}$$

$$Sh_m = 27.9\,Re^{0.376}AR^{-0.656} \quad \text{for both walls.}$$

The Sherwood numbers obtained experimentally were in good agreement with those predicted from the correlations obtained numerically.

Acknowledgements—The authors are indebted to the Korea Science and Engineering Foundation for their partial support of this research.

REFERENCES

1. L. H. Shaffer and M. S. Mintz, Electrodialysis, in *Principles of Desalination* (edited by K. S. Spiegler) pp. 249–352. Academic Press, New York (1966).
2. A. Solan, Y. Winograd and U. Katz, An analytical model for mass transfer in an electrodialysis cell with spacer of finite mesh, *Desalination* **9**, 89–95 (1971).
3. I. S. Kang and H. N. Chang, The effect of turbulence promoters on mass transfer—Numerical analysis and flow visualization, *Int. J. Heat Mass Transfer* **25**, 1167–1181 (1982).
4. G. Belfort and G. A. Guter, An experimental study of electrodialysis hydrodynamics, *Desalination* **10**, 221–262 (1972).
5. A. A. Sonin and M. S. Isaacson, Optimization of flow design in forced flow electrochemical systems, with special application to electrodialysis, *I/EC Process Des. Dev.* **13**, 241–248 (1974).
6. M. S. Isaacson and A. A. Sonin, Sherwood number and friction factor correlations for electrodialysis systems, with application to process optimization, *I/EC Process Des. Dev.* **15**, 313–321 (1976).
7. H. Miyashita, A. Takayanagi, Y. Shiomi and K. Wakabayashi, Flow behavior and augmentation of mass transfer rates using a turbulence promoter in rectangular duct, *Kagaku Kogaku Ronbunshu* **6**, 152–156 (1980).
8. J. S. Watson and D. G. Thomas, Forced convection mass transfer: Part IV, Increased mass transfer in an aqueous medium caused by detached cylindrical turbulence promoters in a rectangular channel, *A.I.Ch.E. Jl* **13**, 676–677 (1967).
9. J. K. Aggarwal and L. Talbot, Electro-chemical measurements of mass transfer in semi-cylindrical hollows, *Int. J. Heat Mass Transfer* **22**, 61–75 (1979).
10. A. K. Runchal, Mass transfer investigation in downstream of sudden enlargement of a circular pipe for very high Schmidt numbers, *Int. J. Heat Mass Transfer* **14**, 781–792 (1971).
11. D. J. Tagg, M. A. Patrick and A. A. Wragg, Heat and mass transfer downstream of abrupt nozzle expansions in turbulent flow, *Trans. Instn Chem. Engrs* **57**, 176–181 (1979).
12. A. A. Wragg, D. J. Tagg and M. A. Patrick, Diffusion-controlled current distributions near cell entries and corners, *J. Appl. Electrochem.* **10**, 43–47 (1980).
13. C. S. Lin, E. B. Denton, H. S. Gaskill and G. L. Putnam, Diffusion-controlled electrode reactions, *Ind. Engng Chem.* **43**, 2136–2143 (1951).
14. M. Eisenberg, C. W. Tobias and C. R. Wilke, Ionic mass transfer and concentration polarization at rotating electrodes, *J. Electrochem. Soc.* **101**, 306–320 (1954).
15. P. H. Bradley, J. L. Greatorex and F. B. Leitz, Effect of turbulence promoters on local mass transfer, OSW Contract No. 14-01-0001-2174 (1970).
16. G. R. Youngquist, An entrance region mass transfer experiment, *Chem. Engng Educ.* **13**, 20–25 (1979).
17. P. P. Grassman, Application of the electrolytic method—I. Advantage and disadvantages, mass transfer between a falling film and the wall, *Int. J. Heat Mass Transfer* **22**, 795–798 (1979).
18. J. J. McFeeley, The response of a diffusion-controlled electrode to pulsed laminar flow, Ph.D. Dissertation, Polytechnic Inst. Brooklyn, New York (1972).
19. I. M. Kolthoff and R. Belcher, *Volumetric Analysis*, Vol. III. Interscience, New York (1957).
20. E. J. DeBeer and A. M. Hjort, Employment of potassium ferrocyanide in standardization of dilute potassium permanganate, *Ind. Engng Chem. Anal.* **7**, 120–121 (1935).
21. I. M. Kolthoff and E. A. Pearson, Stability of potassium ferrocyanide solutions, *Ind. Engng Chem. Anal.* **3**, 381–382 (1931).
22. A. M. Sutey and J. G. Kundsen, Effect of dissolved oxygen on the redox method for the measurement of mass transfer coefficients, *I/EC Fundamentals* **6**, 132–139 (1967).
23. L. Gordon, J. S. Newman and C. W. Tobias, The role of ionic migration in electrolytic mass transport: diffusivities of $Fe(CN)_6^{3-}$ and $Fe(CN)_6^{4-}$ in KOH and NaOH solutions, *Ber. Bunsen. Phys. Chem.* **70**, 414–420 (1966).
24. V. G. Levich, *Physicochemical Hydrodynamics*, pp. 162–171. Prentice-Hall, New York (1962).

ETUDE EXPERIMENTALE DU TRANSFERT MASSIQUE AUTOUR D'UN PROMOTEUR DE TURBULENCE PAR LA METHODE ELECTROCHIMIQUE

Résumé—Le transfert massique local autour d'un promoteur de turbulence dans un canal ayant la géométrie du type zigzag ou du type cavité a été mesuré par la technique électrochimique du courant limite.

Les résultats expérimentaux montrent que les promoteurs de turbulence sont efficaces en brisant la couche limite de concentration et qu'ils accroissent ainsi le transfert. Dans les expériences, le nombre de Reynolds varie entre 10 et 200 pour différents rapports de forme égaux à 3,5, 5 et 7. Les nombres de Sherwood obtenus sont comparés à ceux obtenus numériquement par Kang et Chang. On trouve qu'ils sont compatibles avec une erreur inférieure à 20%.

EXPERIMENTELLE UNTERSUCHUNG DES STOFFÜBERGANGS AN EINEM TURBULENZPROMOTOR NACH DEM GRENZSTROMVERFAHREN

Zusammenfassung—Der örtliche Stoffübergang an einem Turbulenzpromotor in einem Kanal mit Zickzack- oder Kammergeometrie, die durch die Lage der Promotoren bestimmt wird, wurde nach dem Grenzstromverfahren gemessen.

Die experimentellen Ergebnisse zeigten, daß Turbulenzpromotoren wirkungsvoll sind, indem sie die Konzentrationsgrenzschicht aufbrechen, und daher der Stoffübergang zunimmt. Im vorliegenden Experiment wurden die Reynolds-Zahlen von 10 bis 200 variiert für die verschiedenen Seitenverhältnisse von 3,5; 5 und 7. Die experimentell ermittelten Sherwood-Zahlen wurden mit den von Kang und Chang numerisch berechneten Zahlen verglichen. Als Ergebnis wurde eine Übereinstimmung innerhalb einer Fehlergrenze von 20% gefunden.

ЭКСПЕРИМЕНТАЛЬНОЕ ИССЛЕДОВАНИЕ МАССОПЕРЕНОСА ЗА ТУРБУЛИЗАТОРОМ МЕТОДОМ ПРЕДЕЛЬНОГО ТОКА

Аннотация—Методом предельного тока измерены скорости локального массопереноса за турбулизатором, помещенным в канал с геометрией типа зигзаг или полость, в зависимости от местоположения турбулизаторов. Экспериментальные исследования показали, что турбулизаторы могут эффективно использоваться для разрушения концентрационного пограничного слоя и тем самым увеличения скорости массопереноса. В проведенных экспериментах числа Рейнольдса изменялись в диапазоне от 10 до 200 при различных отношениях сторон: 3,5; 5 и 7. Полученные экспериментальные значения числа Шервуда сравнивались со значениями, рассчитанными численно Кангом и Чангом. В обоих случаях погрешность не превышала 20%.